Investigating Electrochemical Behavior of Antibacterial Polyelectrolyte-Coated Magnesium Alloys for Biomedical Applications

M.S. Seraz[1], M.N. Uddin[1], S.Y. Yang[2] and R. Asmatulu[1,*]

[1]Department of Mechanical Engineering; [2]Department of Biological Science, Wichita State University, 1845 Fairmount, Wichita, KS 67260, USA

Abstract: This study presents corrosion rates of layer-by-layer (LBL) and self-assembled monolayer (SAM) coated magnesium (Mg) alloys, and their antibacterial properties. Mg alloy samples were coated with cationic (chitosan - CHI) and anionic polyelectrolyte (carboxymethyl cellulose-CMC) LBL coating, and phosphonic acid self-assembled monolayer (SAM) coating methods. Electrochemical impedance spectroscopy (EIS) was employed for analyzing these samples in order to detect their corrosion properties. During the electrochemical analysis, a corrosion rate of 72 milli inch per year (mpy) was found for the sample coated with a 12 deionized phosphonic acid SAM and 9 CHI/CMC multilayers. During the antibacterial tests, gentamicin was investigated about how it would adhere on the Mg substrate surface and how it would be an antibacterial agent against *Escherichia coli* (*E. coli*) bacteria. From a coating point of view, a bare layer, self-assembly monolayer, polyelectrolyte layer, and combination of LBL and SAM were analyzed. From an antibacterial treatment point of view, samples with no antibacterial treatment, 10% gentamicin sulfate, UV treatment and 0% gentamicin sulfate, anti-anti and 10% gentamicin sulfate, and 70% ethanol and 10% gentamicin sulfate were individually studied. Duration of the incubation was 7 days at 35°C. Antibacterial sensitivity was tested using the disk diffusion method in Petridish. Based on the standard diameter of the zone of inhibition chart, the growth of bacteria was inhibited relatively with those Mg substrates. The largest recorded diameter of the zone of inhibition was 50 mm for the pre-UV treated and gentamicin-loaded sample, which is more than the standard inhibition diameter.

Keywords: Magnesium Alloys, Polyelectrolyte Layer Coatings, Corrosion Rate, Antibacterial.

1. INTRODUCTION

Magnesium (Mg) is one of the most studied metals for cardiovascular applications for stent and other biodegradable implants. It has a systemic toxic level of about 7 to 10 mill moles per liter of serum [1]. The basis for using Mg as a biodegradable stent material is that it is an element of the tissue structure of many living organisms, and as a substantial intracellular cation, Mg is part of more than 300 biological reactions in a cell. Mg is also non-carcinogenic. Addition of Ca and Zn into Mg alloys should be limited to 2 wt.% and 6 wt.%, respectively, considering the corrosion properties of Mg alloy [2]. Extensive research has been performed for the use of Mg and its commercially available alloys for biomedical applications [3]. It takes priority over other biodegradable materials because of some basic biomedical properties [4-6]. However, Mg degrades rapidly in aggressive chloride environments, such as human body fluid. Rapid degradation of Mg implants results in tissue overloaded with degradation products, which can lead to neointimal formation [1].

Mg alloys were experimented on earlier in an *in vivo* study to determine if they were suitable for orthopedic applications. The study was conducted on rabbit tibiae, whereby Mg alloys (LAE442, WE43, MgCa0.8, AX30, and ZEK100) were implanted into rabbit tibia, and the mechanical strength, *in vivo* corrosion rate, and biocompatibility were examined. A higher mineral apposition rate (MAR) was found in the examined groups with Mg implants than the control tibiae, so the bone remodeling was better with the Mg implant. Especially in the first month, the MAR was 4.29 μm/d in the MgCa0.8 group and 3.36 μm/d in the LAE442 group, which is higher than in the control group without implant material (MAR 0.87 μm/d) [7]. These results opened up the new doors for using Mg alloys in orthopedic applications. Today, some of orthopedic screws, plates, and rings are produced from Mg alloys.

Currently, stent application (the ureteral stent) involving the Mg alloy has been in progress. Clinical complications and failure of indwelling medical devices are the consequences of bacterial infection. This is especially noticeable in the case of ureteral stents, which are the current clinical solution to treating blockage in arterial canals. Commonly, this type of stent, which is currently made of polyurethane, can be infected with *Escherichia coli* (*E. coli*) bacteria. Incubating *E. coli* with Mg samples has resulted in a decrease in the bacterial cell density, compared with the currently used commercial polyurethane stent [8]. Clinically, Mg will be the better choice of materials out of which to make this ureteral stent. Mg degradation in immersion solutions (artificial urine, Luria Bertani broth, and deionized water) has resulted in an alkaline pH shift.

*Address correspondence to this author at the Department of Mechanical Engineering, Wichita State University, 1845 Fairmount, Wichita, KS 67260, USA; Tel: (316) 978-6368; Fax: (316) 978-3236;
E-mail: ramazan.asmatulu@wichita.edu

E-ISSN: 2311-8741/17 © 2017 Savvy Science Publisher

Lately, focusing on bacterial infection issues in the case of a magnesium implant application, the effects of Mg metal with increased Mg^{2+} concentration and alkaline pH were analyzed on the *in vitro* growth of *E. coli*, *Pseudomonas aeruginosa*, and *Staphylococcus aureus* in three separate experiments [9]. The increments in pH and Mg^{2+} concentration were predictable, regardless of the quantity of Mg added, so it is possible to obtain antibacterial effects, similar to that of fluoroquinolone antibiotics, by adding Mg and increasing the pH value. The mechanism that results in an antibacterial effect of Mg on three common aerobic bacterial organisms is the alkaline pH [10].

A group of researchers have studied the antibacterial behavior of Mg based metal, pure Mg, and AZ31 alloy, with and without surface coatings. The results of those studies have indicated that both pure Mg and AZ31 alloy had a strong antibacterial effect against *E. coli*. Antibacterial ability has been found in cases of pure Mg with a porous silicon (Si)-contained coating by micro-arc oxidation (MAO) maintaining a mild increase in the pH value. However, fluorine-contained (F) pure Mg and Si-coated AZ31 alloy lost their antibacterial abilities with almost no change in pH values because of the less-porous coatings on the surfaces. The results of this work indicate that surface coating could have a strong effect on the antibacterial ability of Mg-based metals. A Mg and silicon coating by MAO showed antibacterial ability with a mild increase in the pH value due to the porous structure of the coating [11]. On the other hand, Mg with F and the AZ31 alloy with Si coatings using chemical conversion coating method resulted in non-antibacterial surface at almost the same pH value [12]. This occurs because of more dense coatings on metal surfaces. Therefore, a porous coating on Mg-based metals is expected to not only reduce the degradation rate to some extent but also have an additional antibacterial activity, which has a potential clinical value in practice.

This project investigates the corrosion properties of Mg alloys with a polyelectrolyte coatings and measurement of antibacterial sensitivity of gentamicin against *E. coli* and reinforcing the antibacterial sensitivity of gentamicin by using a secondary antibacterial agent or treatment. The novelty of the project is that layer-by-layer coatings and self-assembled monolayer coatings associated with antibacterial agents were applied on the surface of magnesium alloy to control the electrochemical properties and improve the biomedical applications of these new materials.

2. EXPERIMENTAL

2.1. Materials

Cationic (chitosan-CHI) and anionic polyelectrolytes (carboxymethyl cellulose-CMC), dimethyl sulfoxide (DMSO), acetic acid, ethanol, and phosphate buffer solution (PBS) capsules were purchased from Sigma Aldrich. Gentamicin sulfate, antimycotic (anti-anti) and other items were locally provided. Electrochemical impedance spectroscopy (EIS) and antibacterial sensitivity tests were performed on the Mg alloy (AZ31).

2.2. Methods

2.2.1. SAM and Polyelectrolyte Coatings

The SAM coating procedure involving a 2 mM solution of 12 Di-PA in DMSO is as follows: the Mg alloy samples were ultrasonically cleaned for 10 minutes each in acetone and ethanol and rinsed with DI water and DMSO three times. Then, the samples were immersed in the SAM solution for the next 48 hours in a water bath kept at 35°C. When a SAM layer formation is complete, the samples were rinsed with acetone and DI water following the air drying. For the polyelectrolyte coating, a chitosan solution was prepared from 1.5 g of chitosan in 1,000 ml of DI water with 5 ml of acetic acid. A CMC solution was also prepared from 1.5 g of CMC in 1,000 ml of DI water. For the LBL dip-coating, the bare Mg or SAM-coated Mg substrate was immersed in cationic polyelectrolyte (chitosan) for 10 minutes followed by rinsed in DI water for another 6 minutes. The substrate was then immersed in anionic polyelectrolyte (CMC) for 10 minutes. Finally, the substrate was rinsed again with DI water for 6 minutes.

Figure **1a** shows the above sequence of LBL formation by dip coating, which is how a single layer is formed by electrostatic bonding between positive and negative sub layers of chitosan and CMC, respectively [13]. If more layers are needed, then the process is repeated. The samples were placed inside the biological safety cabinet for 1 hour. The Thermo Scientific 1300 Series A2 biological safety cabinet was used for the UV treatment purposes. Both surfaces of the samples were exposed to the UV light for 30 minutes on each side.

2.2.2. Gentamicin, Anti-Anti and Ethanol Loadings

A simple vacuum desiccator was used as the vacuum chamber. The air inside of the desiccator was

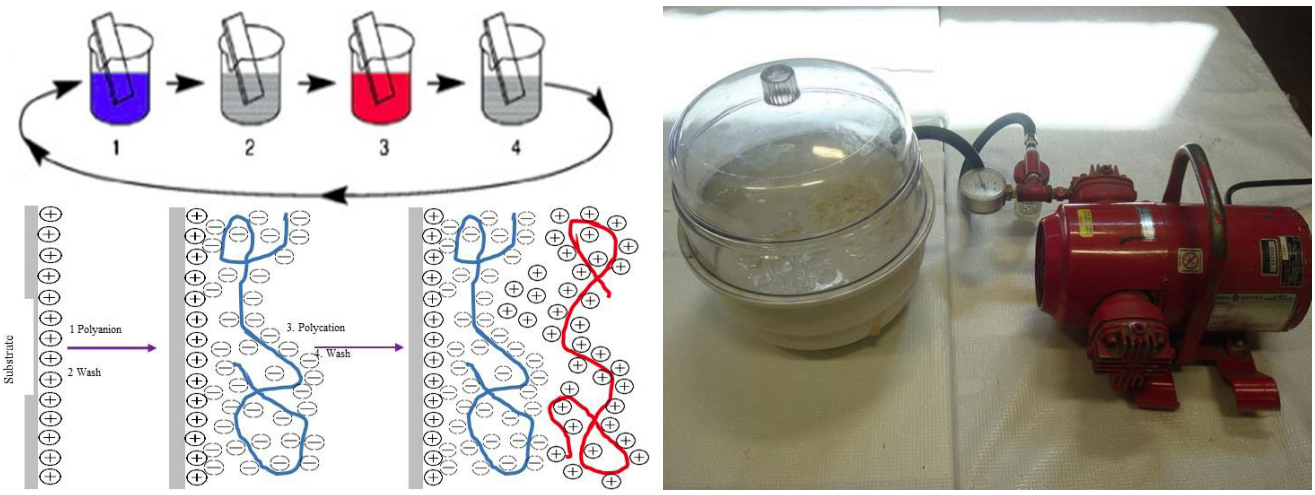

a **b**

Figure 1: a) LBL assembly by dip coating on a substrate [13], and **b**) gentamicin sulfate loading on Mg substrates in vacuum chamber.

pumped out using a vacuum pump. Each single sample was placed in a single beaker containing the 10% gentamicin sulfate solution in DI water. Then, all beakers containing the Mg sample immersed in the gentamicin sulfate solution were put in the vacuum desiccator. The beakers with solutions and samples were left inside the vacuum chamber for 30 minutes. Then, all samples were taken out of the solution and air dried. Figure **1b** shows the vacuum loadings / absorptions on the Mg substrates. Some of the samples were immersed in the anti-anti solution, while some in 70% ethanol. This process is similar to gentamicin loading, but conducted in a sterile condition inside a biological safety cabinet instead of using a vacuum. The anti-anti or ethanol loaded samples were loaded with gentamicin in a sterile, but not vacuum condition. For all results, the diameter of the zone of inhibition was measured after seven days of incubation.

2.2.3. Bacteria Medium Preparation

Miller broth in the amount of 25 mg was diluted with 1,000 ml of DI water to form a 2.5 % LB dilution. For every single petri dish, 200 microliters of the LB dilution were used. The dilution changed to gel overnight, and the bacteria were cultured in a tube containing 0.25% solution of Miller broth. Samples were placed on a gel medium after the bacteria were seeded over the entire plate. All petri dishes were incubated at 37°C and kept there for a maximum of 10 days.

3. RESULTS AND DISCUSSION

3.1. Surface Characterization

The characterization tests were performed on the prepared samples before the EIS analyses. A number of SEM images based on different types of SAM solutions, number of layers, and heat treatment were taken. Then, all samples were tested with EIS. Figure **2** shows the SEM images of effects of increasing the polyelectrolyte layers on the surfaces of 16 PA-coated and 12 Di-PA-coated samples at room temperature.

In both cases, it was found that the SAM layer provided better fineness/quality over the surface of the substrate. This surface fineness indicates the SAM's effectiveness as a surface modification method. The polymer layers also appeared smooth. No other surface irregularity was observed on these sets of prepared samples. It also showed that the 16 PA SAM and 9-layer-coated sample had some small cracks on the surface, while the 12 Di-PA sample had no cracks at the same magnification. Hence, it can be concluded that the 16 PA SAM layer does not bind to the cationic polyelectrolyte layer (chitosan) as strongly as does 12 Di-PA SAM. The 12-Di PA sample has a phosphate tail on each end, while 16 PA has only one tail. Therefore, the attachment between chitosan and 12 Di-PA is stronger than that between chitosan and 16 PA. This could be the possible reason for the crack in 16 PA-coated samples.

Figure **3** illustrated the effects of heat treatment on the surfaces of the samples. Heat treatment significantly reduced porosity of the polyelectrolyte layers. The porosity of the non-heat treated sample may be because of the trapped air in the polyelectrolyte layers, which were bubbled up during the heat treatment and air expansion between the layers. Otherwise, heat treatment might not significantly change the surface fineness and quality.

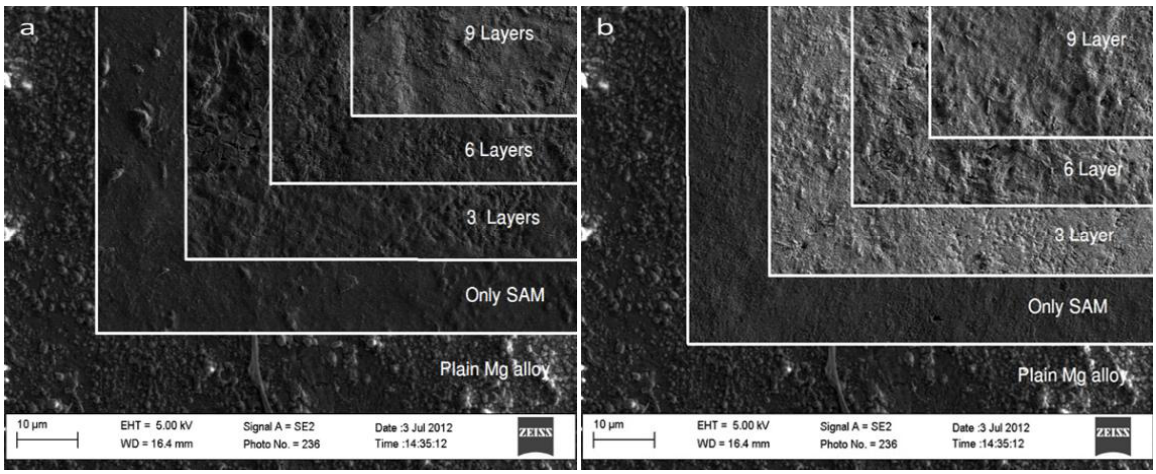

Figure 2: SEM images of contrast of (**a**) 16 PA SAM-coated samples, and (**b**) 12 Di-PA SAM coated samples.

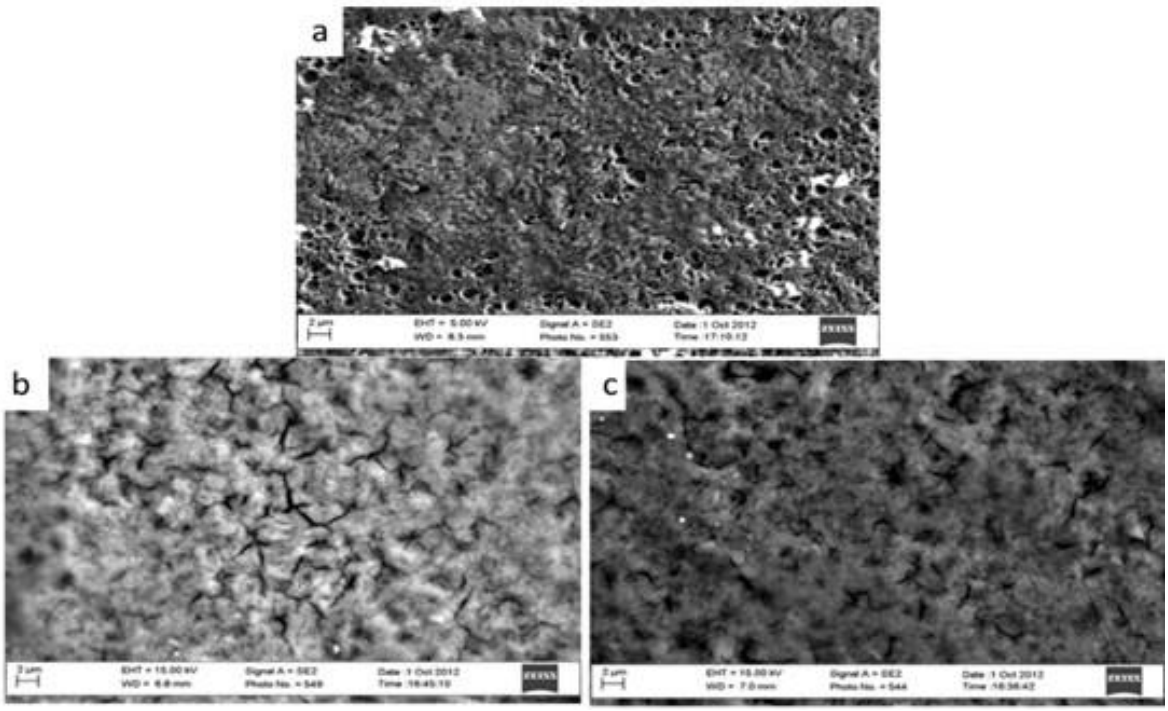

Figure 3: SEM images of 12 Di-PA and 9 multilayer-coated samples at **a**) room temperature, and after **b**) 80°C and **c**) 125°C heat treatments.

3.2. Electrochemical Analysis

In the first set of the EIS tests, a number of Nyquist studies were conducted on the various types of non-heat treated samples. The Nyquist curves indicated that the coating failure patterns were almost similar for the samples prepared using the same conditions. It is important to mention that the 3 multi-layered samples deviated from the gradual decrement rate of corrosion, with a big difference between 12-Di PA and 16 PA SAM. Although the decrement of corrosion rate was not significant according to the requirement of corrosion resistance, LBL polyelectrolyte layers generally decreased the corrosion rates. This may be because of the weak corrosion resistances of the LBL coated samples. Surprisingly, for the sample with 16 PA SAM only, the corrosion rate was higher than bare Mg alloy sample. This deviation is statistically valid for each type of coating, because at least three samples were conducted and a similar result was found each time. The reason for such a drastic decrement of corrosion rate is yet to be investigated.

Figure **4** shows the Tafel curves of non-heat treated 16 PA SAM-coated and 12 Di-PA SAM-coated samples. As can be seen, the Tafel curve for 16 PA

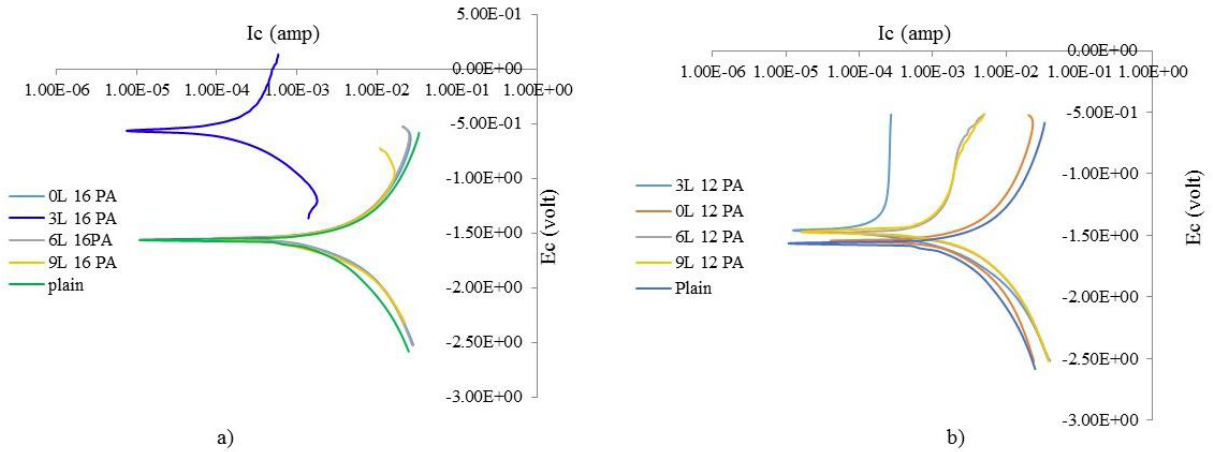

Figure 4: Tafel curves of non-heat treated samples for a)16 PA SAM-coated and b) 12 Di-PA SAM-coated Mg samples.

SAM- and 3 layers-coated sample is quite deviated from the others; however, the patterns of Tafel curves for the 12 Di-PA samples are quite close to each other (Figure **4b**). Otherwise, the corrosion rate behaved inversely with the increased number of polyelectrolyte layers. Therefore, this study concluded that a combination of CHI/CMC coating is fairly weak against simulated body fluid or phosphate buffer saline. Figure **5** shows the comparison of corrosion rates among non-heat-treated samples based on the Tafel curves.

Fekry *et al*. reported the electrochemical behaviors of two extruded AZ31E and AZ91E alloys in the PBS solution of pH 7.4 at 37°C using EIS technique [14]. Polarization measurements were carried out to study the corrosion rate, which confirmed with EIS unit that the corrosion resistance of the AZ91E alloy is higher than that of the AZ31E alloy. Also, the effect of adding 10^{-3} M concentration of 2-thiouracil and L-tyrosine as an inhibitor in the PBS solution for AZ91E alloy was studied, and it was found that the corrosion was inhibited more with the addition of L-tyrosine than with 2-thiouracil. Corrosion resistance of the AZ31E alloy increases with immersion time in the PBS solution for 24 hours; then, it decreases sharply after five days of duration. Corrosion resistance of the AZ91E alloy increases with immersion time in the PBS solution for three days, at which time it decreases sharply until five days. Corrosion resistance of the AZ91E alloy is much better than that of the AZ31E alloy in the PBS solution. Corrosion of the AZ91E alloy in the blank can be effectively inhibited by the addition of 1 mmol 2-thiouracil or 1 mmol L-tyrosine. However, L-tyrosine is much more effective than 2-thiouracel as an inhibitor. Polarization results strongly confirm the impedance data. The results of the present experiment conform to the results found in the EIS study for the AZ31 sample [14].

The structure and properties of the composite membranes were investigated by Fourier transform infrared spectroscopy, x-ray diffraction, scanning electron microscopy, mechanical performance measurement, swelling behavior test, and a soaking behavior study in phosphate buffered saline and simulate body fluid [15]. Results of those experiments

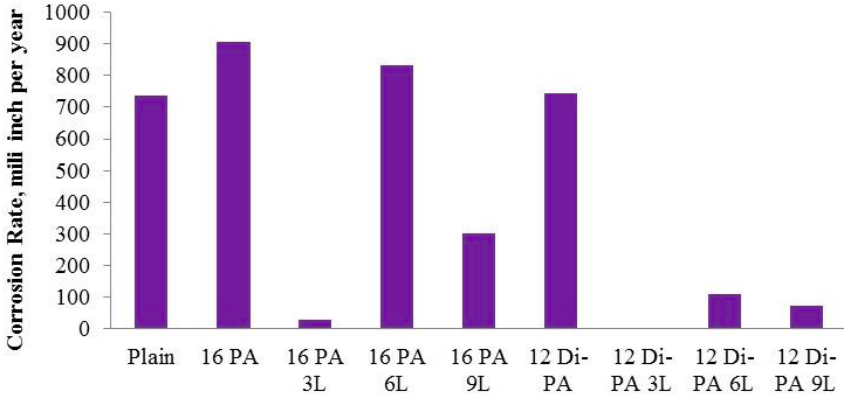

Figure 5: Comparison of corrosion rates for non-heat treated samples based on the Tafel curves.

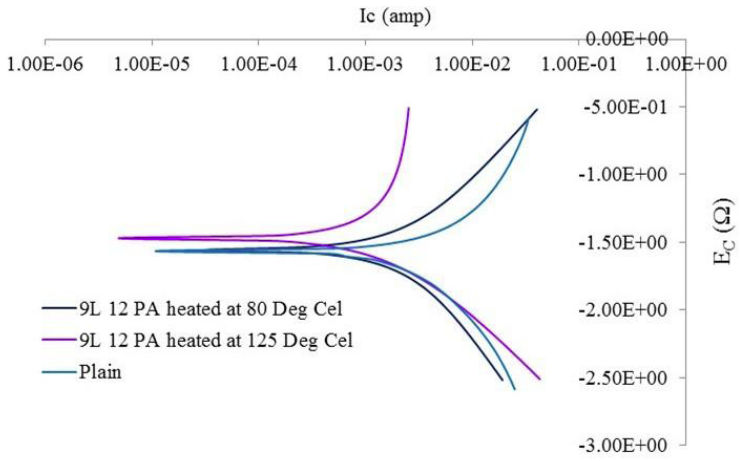

Figure 6: Tafel overlay of heat treated samples at 80°C and 125°C, and plain sample at room temperature.

showed that the n-HA/CHI/CMC composite membrane was formed though a superficial static electricity interaction among n-HA, CHI, and CMC. For the n-HA/CHI/CMC composite membrane, the microstructure compatibility, mechanical property, swelling behavior, degradation, and bioactivity *in vitro* of the composite membrane were improved with the addition of n-HA, compared to the CHI/CMC polyelectrolyte complex membrane. Moreover, the n-HA/CHI/CMC composite membrane with 40 wt.% n-HA had the highest mechanical property, which suggested that the novel n-HA/CHI/CMC composite membrane with 40 wt.% n-HA was more suitable for use as a guided bone tissue regeneration membrane than a CHI/CMC polyelectrolyte complex membrane. In addition to the necessity of hydroxyapatite in the coating combination, one property of the polyelectrolyte is also highly desirable. This property is the di-electric constant. In the EIS analysis, much of the impedance is expected from capacitive reactance. Capacitive reactance is the part of total circuit impedance that is produced by the polyelectrolyte coating. The optimization of the polymer's di-electric constant, the number of coating layers, and the application of hydroxyapatite will ensure the expected scale of corrosion resistance against human body fluid.

Figure **6** shows the Tafel overlay of heat treated samples at 80°C and 125°C, and plain sample at room temperature. From Figure **6**, it can be seen that the corrosion current of the heat-treated samples is smaller in magnitude than the corrosion current of the bare sample at room temperature. Comparing the results of heat treated samples with non heat treated one, it can be seen that the heat-treated sample shows a higher corrosion rate (322 mpy at 80°C and 292.78 mpy at 125°C) compared to that of the non-heat-treated (72 mpy) sample. As is found earlier in the SEM images, heat treatment reduced the porosity of the coating layers, and better corrosion resistance was expected. Simultaneously, the main purpose of heat treatment was to create cross-linking between the polyelectrolytes. However, results showed the opposite situation. The reason behind this phenomena may be because of the defects formations on the nanofilms of the Mg alloys and thermal shrinkages. Thus, this behavior could be a future matter of investigation.

3.3. Antibacterial Sensitivity Tests

The antibacterial effect of gentamicin sulfate-loaded Mg alloys can be determined by measuring the zone of inhibition, which is the standard way of measuring it in the disk-diffusion method [24]. When a disk of anti-bacteria is put on the plate where bacteria grow in a proper medium, a circular zone of inhibition, through which bacteria cannot trespass, appears around the disk. By measuring the diameter of the zone and checking with the Standard Antibiotic Susceptibility Zone Diameter Measurement Chart, a decision about the antibacterial effect of the disk can be reached—whether it is resistant, intermediate, or susceptible [16,17]. The following results are described in order, based on the type of antibacterial treatment coating on the Mg alloy substrate. Figure **7** shows the petri dish containing samples with different antibacterial treatment coating on the Mg alloy substrate in a bacteria medium. All the images were taken after 7 days of incubation at 37°C. Typically on day zero, all petri dishes were visually the same regarding bacteria growth.

As is shown in Figure **7b**, the petri dish surface has been infected thoroughly with E. coli due to the lack of

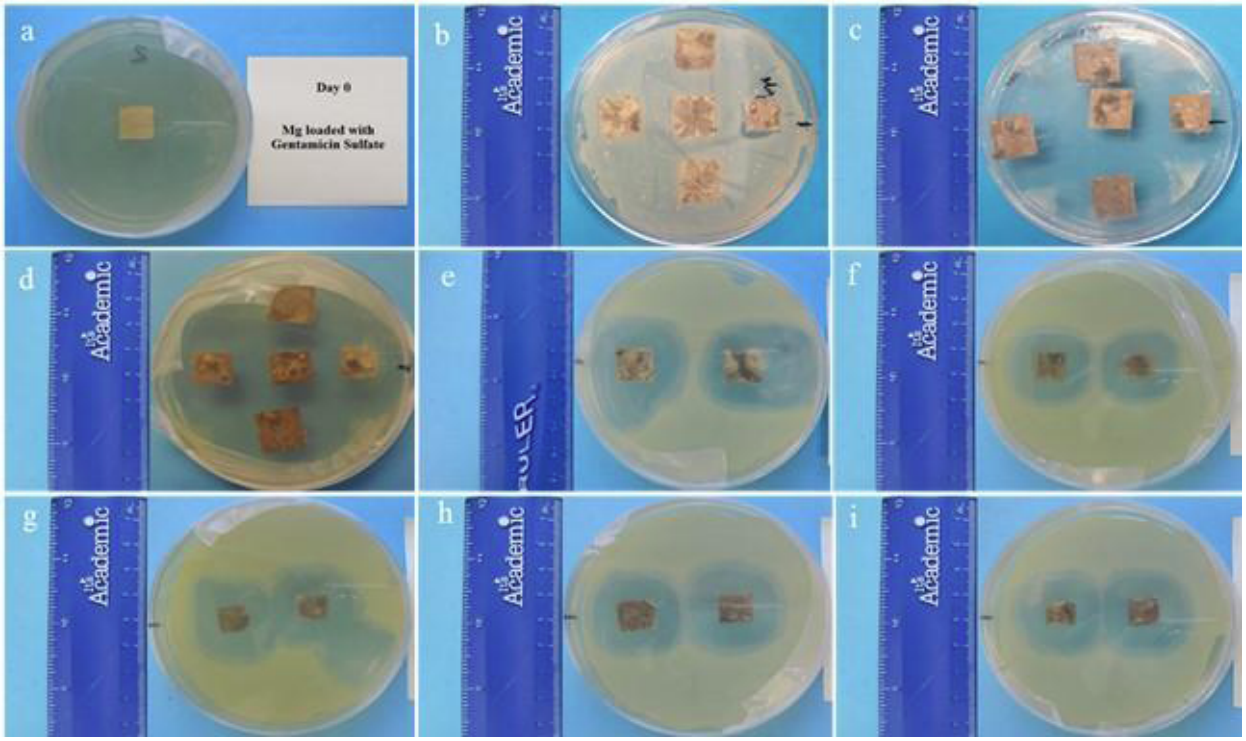

Figure 7: Petri dish containing samples in a bacteria medium on (**a**) day zero, (**b**) without antibacterial treatment, (**c**) with gentamicin sulfate, (**d**) UV-treated and gentamicin-loaded, (**e**) bare magnesium with ethanol and gentamicin sample (left) and anti-anti gentamicin sample (right), (**f**) PE- and SAM-coated sample with anti-anti and gentamicin (right), (**g**) PE-coated sample with anti-anti and gentamicin (right), (**h**) PE- and SAM-coated samples with ethanol and gentamicin sulfate (right), and (**i**) PE-coated samples with ethanol and gentamicin sulfate (right).

the antibacterial treatment. It was a matter of interest to see if polyelectrolytes and SAM could produce any antibacterial resistance in the case of the coated samples. Results showed no signs of that occurring. Figure **7e** shows two samples on a petri dish. None of these samples were polyelectrolyte- or SAM-coated. The left-hand sample was loaded with a combination of 70% ethanol-gentamicin, and the right-hand sample was loaded with a combination of anti-anti - gentamicin. The zones of inhibition are clearly visible on the petri dish surface. The yellowish portion of the petri dish is infected and the rest is not. In both cases, the samples were loaded under a sterile non-vacuum condition inside a biological safety cabinet. The sample coated with a combination of 6 polyelectrolyte layers and 12 Di-PA SAM is shown on the right hand side of the petri dish in Figure **7f**. This sample was loaded with a combination of anti-anti and gentamicin in a sterile non-vacuum condition. From Figure **7f**, it's found that the right-hand sample is similar to the one shown in Figure **7g**, but it is coated with only 6 polyelectrolyte layers. Similar finding is observed in PE- and SAM-coated samples with ethanol and gentamicin sulfate and PE-coated samples with ethanol and gentamicin sulfate. Figure **8** shows the comparison of the zone of inhibition diameter of all the samples irrespectively.

Figure **9** shows the comparison of zone of inhibition diameter among only gentamicin, combination of gentamicin and anti-anti and combination of gentamicin and ethanol. From Figure **9**, we find that Gentamicin and UV treatment and Gentamicin and Anti-Anti loaded samples exhibit no antibacterial resistance at all for the samples, either bare or coated with polyelectrolyte and SAM. However, it was a matter of interest to observe, if polyelectrolyte-coated samples provide any antibacterial resistance or not. It is already established that a water-soluble chitosan (43 kDa) was found to be the most effective one against *E. coli* O157:H7 and Salmonella enteric, especially using the agar dilution method [18]. *In vitro* antimicrobial activities of the obtained chitosan-metal complexes, which were found to be much better than free chitosan and metal salts, were examined against two Gram-positive bacteria (*S. aureus* and *S. epidermidis*), two Gram-negative bacteria (*E. coli* and *P. aeruginosa*) and two fungi (*C. albicans* and *C. parapsilosis*). The test results indicated that the inhibitory effects of chitosan-metal complexes were dependent on the property of metal ions, the molecular weight and degree of deacetylation of chitosan and environmental pH values [19]. Electro-microscopy confirmed that the exposure of *S. auresus* to the chitosan-Cu (II) complex resulted in the

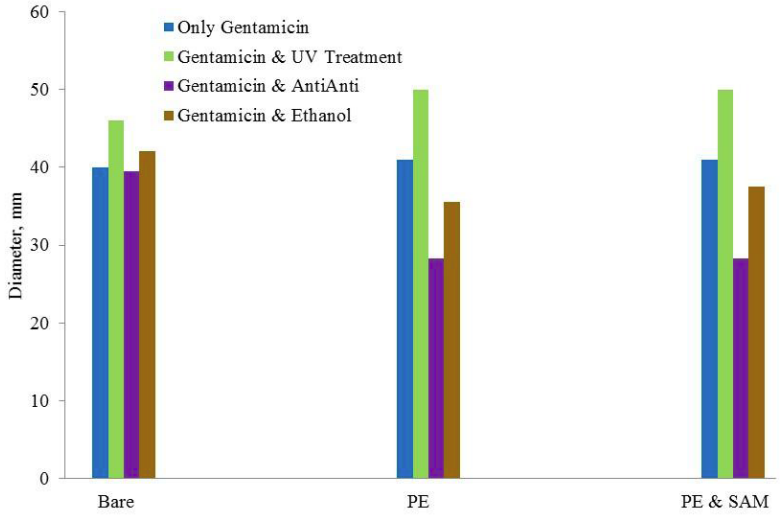

Figure 8: Comparison of the zone of inhibition diameter of the Mg samples.

disruption of cell envelop. Based on the discussion of the antimicrobial mechanism of chitosan-metal complexes and their molecular structures, the structure-activity correlation for the antimicrobial activities was elucidated. At the same time, It is known that the chitosan/CMC bond is an electro-static bond [20].

There is a strong possibility that the electrostatic bond also prevented chitosan from making a hydrogen bond with the ribosomal subunits. It stated that in or to resist bacterial growth, it is needed to have a hydrogen bond between the antibacterial agent and the 16S-rRNA. It is very possible that the presence of an anionic solution made this possibility to decrease. Based on these two observations, interactions between the chitosan-Mg and the chitosan-CMC should be investigated further to produce antibacterial resistance from the chitosan/CMC-coated Mg alloy substrate. As for the rest of the results, it is found that every sample set had a zone of inhibition diameter above 15 mm. Therefore, irrespective of coating type, antibacterial treatment, and sample size, the project to ensure the highest sensitivity of gentamicin sulfate loaded on Mg alloy against *E. coli* was successful. Based on the auxiliary antibacterial treatments followed in our experiment, UV treatment has provided the best possible result (Figure **9**).

Surprisingly, Figure **8** showed that gentamicin sulfate followed by no additional antibacterial treatment takes the next position. Nevertheless, it is expected a better result from the samples having a combination of two antibacterial agents- gentamicin sulfate as the primary one and Anti-Anti or Ethanol as the secondary one. In case of Anti-Anti antibacterial, it is already known that it is a solution containing 10000 units/ml of penicillin, 10000 µg/ml of streptomycin, and 25 µg/ml of amphotericin B. Here, the one to one interactions between streptomycin and gentamicin, amphotericin and gentamicin and penicillin and gentamicin are the first issue under consideration. In the previous experiments, it has been proved that penicillin does not cause any kind of inactivation of gentamicin sulfate at 37°C if the dose is either small or medium [21]. The combination of penicillin and gentamicin may be considered an alternative for the treatment of enterococci endocarditis, especially when penicillin and streptomycin are not synergistic [22]. On the other hand, streptomycin itself is an aminoglycoside, and has no chance of inactivating another aminoglycoside, gentamicin [23-24]. It was expected that the

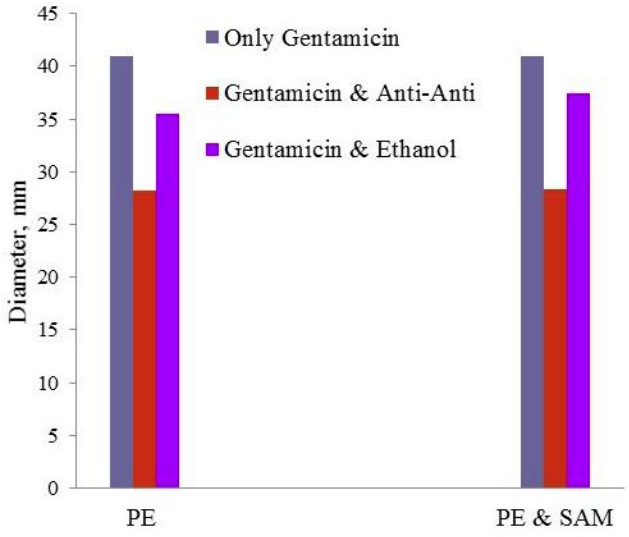

Figure 9: Comparison of zone of inhibition diameter among only gentamicin, combination of gentamicin and anti-anti and combination of gentamicin and ethanol.

combination of multiple antibacterial loaded sample will show stronger resistance. But the combination of gentamicin and anti-anti one behaved weaker. The gentamicin and ethanol one showed small improvement. Therefore, undoubtedly the drug loading condition played a strong role for this unexpected result. The only gentamicin loading was done in vacuum condition and the combined samples were loaded in sterile, but not vacuum condition. Based on this observation, it is indicated that the vacuum condition provides the highest quantity of drug loadable.

Because there is no sign of adverse effects detected, the combination of gentamicin and anti-anti and the combination of gentamicin and ethanol should have produced a stronger antibacterial effect than gentamicin alone. In case of polyelectrolyte-coated samples (Figure **9**), the interaction between the polyelectrolytes and the antibacterial drugs used could be a reason for the weaker antibacterial function of the polyelectrolyte-coated samples loaded with combination drugs. It is clearly concluded that incorporation of chitosan into gentamicin-loaded bone cement for use in joint replacement surgery has no antimicrobial benefit and the detrimental effect on mechanical properties may have an adverse effect on the longevity of the prosthetic joint [25]. It has been investigated whether the incorporation of chitosan in gentamicin-loaded bone cement increases antibiotic release, and prevents bacterial adherence and biofilm formation by clinical isolates of Staphylococcus spp. Different amounts of chitosan were added to the powder of the gentamicin-loaded bone cement. Gentamicin release was determined using high-performance liquid chromatography mass spectrometry. Bacterial adherence and bacterial biofilm formation were determined using clinical isolates cultured from implants retrieved at revision hip surgery.

In this study, the best result was found from the UV treated and Gentamicin loaded Mg samples. The lowest zone of inhibition diameter recorded was 46 mm for bare sample and the highest one was more than 50 mm for PE and SAM-coated sample. Ultraviolet (UV) light is well established as a light inactivation treatment,

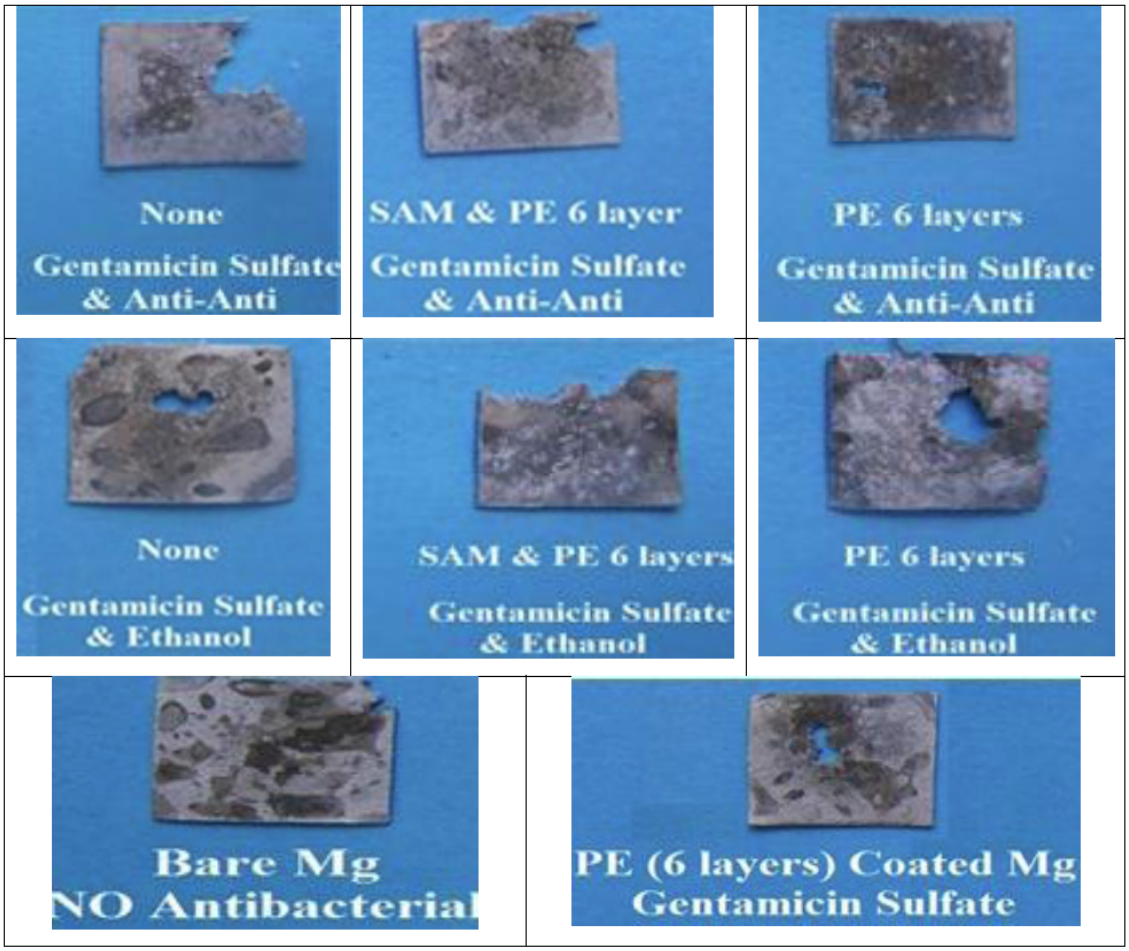

Figure 10: Mg degradation samples for (top raw) Gentamicin and Anti-Anti loaded; (middle raw) Gentamicin and Ethanol loaded; and (bottom raw) Bare sample without any drug and PE-coated sample with gentamicin sulfate.

inducing effects ranging from DNA damage, primarily as a result of UV absorption by DNA at wavelengths of 240 nm to 280 nm, to sub lethal damage of DNA repair systems caused by near-UV light. Our samples were UV treated before getting loaded with gentamicin sulfate. The purpose of treating our samples with UV light is to eliminate any existing microorganisms that can accelerate the growth of bacteria or fungi. Some previous study concluded that the use of UV treatment is the most effective in aquaculture [26]. In our cases, we did the UV treatment of dry samples, and it is the same experiment of reference [26], ensuring that the UV treatment leaves some residual microorganism as well. Furthermore, recent work has shown that photosensitization of bacterial cells is independent of the antibiotic resistance spectrum [27,28]. Recent studies are in progress to ensure the same microbial inactivation without any additional photosensitization. As visible light does not break the DNA structure, post-antibacterial agent treatment can be possible with or without photo sensitizing to inhibit bacterial growth more effectively.

3.4. Magnesium Disintegration

In the present study, it was observed some disintegration of Mg alloys during the incubation process. Figure **10** illustrate the condition of the samples after 10 days in an incubator at 37°C. The most possible reason for this metal disintegration is the high corrosion rates due to the bacterial medium, which is highly aqueous. The LB bacterial medium was dissolved in 1000 ml of DI water. Thus, the sample was in contact of an aqueous gel continuously during incubation. However, why the disintegration rate is higher in the case of the polyelectrolyte and SAM coating is an issue of further investigation.

4. CONCLUSIONS

The viability of anti-bacterial drug delivery approach for the human body was studied using the Mg alloys. It is a matter of interest if it is possible to ensure strong attachment of the anti-bacterial drug on Mg substrate. In this study, maximum 50 mm diameter of zone of inhibition has been recorded for pre UV treated & gentamicin sulfate loaded Mg substrate against *E. coli* compared to 15 mm of standard requirement. Thereby, immersion in 10% gentamicin sulfate solution inside vacuum condition has been proven as an effective method of anti-bacterial drug loading. It was also found that polyelectrolyte coating created some negative effect on the antibacterial sensitivity of the primary antibacterial agent (gentamicin) and the secondary one (anti-anti or 70% ethanol). Thus, the decision is to use an alternative biocompatible coating that will not hinder the molecular antibacterial mechanism of gentamicin sulfate. Not only the interaction among chitosan/CMC combination, gentamicin sulfate and anti-anti or 70% ethanol, but also the combination of chitosan/CMC produced a very low corrosion resistance against simulated body fluid (PBS). In order to ensure that the implant will last inside the human body for a required period of time, it is needed to use a different combination of cationic and anionic polyelectrolytes. Based on the theory of electrochemistry of the corrosion resistance, the alternative polyelectrolyte combination should have a significantly high di-electric constant. The experimental studies also found that UV treatment of the metal substrate before anti-bacterial loading takes part in increasing the anti-bacterial effect significantly. All these findings make the proper way to produce cardiovascular implant and ureteral stent by UV treated Mg alloy loaded with gentamicin sulfate from a clinical point of view.

REFERENCES

[1] Moravej, M. and Manitoban, D. (2011). Biodegradable Metals for Cardiovascular Stent Application: Interests and New Opportunities. Int J Mol Sci., 12(7), 4250–4270. https://doi.org/10.3390/ijms12074250

[2] Ratner, B. D., Hoffman, A. S., Lemons, J. E. (2013). An Introduction to Materials in Medicine. Biomaterial Science, 3rd Edition, 695-713. https://doi.org/10.1016/B978-0-08-087780-8.00059-0

[3] Groisman, E. A., (2001). Principles of Bacterial Pathogenesis, Academic Press, Elsevier, 12-14.

[4] Mordike, B. L., Ebert, T. (2001). Magnesium: Properties-Applications-Potential. Materials Science and Engineering A, 302 (1) 15, 37–45. https://doi.org/10.1016/S0921-5093(00)01351-4

[5] Staiger, M. P., Pietak, A. M., Huadmai, J., Dias, G. (2006). Magnesium And Its Alloys As Orthopedic Biomaterials: A Review. Biomaterials.1728-1734. https://doi.org/10.1016/j.biomaterials.2005.10.003

[6] Kainer, K. U. (2003). Magnesium Alloy & Technologies. Wiley VCH, 1-2. https://doi.org/10.1002/3527602046

[7] Reifenrath, J., Bormann, D. and Lindenberg, A. M. (2011). Magnesium Alloys as Promising Degradable Implant Materials in Orthopedic Research. University of Hanover, Germany, 93-108.

[8] Lock, J. Y., Draganov, M., Whall, A., Dhillon, S., Upadhyayula, S., Vullev, V.I., Liu, H., (2012). Antimicrobial Properties of Biodegradable Magnesium for Next Generation Ureteral Stent Applications. Conf Proc IEEE Eng Med Biol Soc., 1378-1381. https://doi.org/10.1109/embc.2012.6346195

[9] Pseudomonas: Advances in Research and Treatment. (2012). Scholarly Editions, Atlanta, GA, 38-40.

[10] Robinsona, D. A., Griffithb, R. A., Shechtmanc, D., Evansd, R.B., Conzemiusa, M.G. (2010). *In vitro* Antibacterial Properties of Magnesium Metal Against Escherichia coli, Pseudomonas aeruginosa And Staphylococcus aureus. Acta Biomaterialia, 6(5) 1869–1877. https://doi.org/10.1016/j.actbio.2009.10.007

[11] Xue-Nan, G.U., Yu-Feng, Z. (2010). A Review on Magnesium Alloys As Biodegradable Materials. Front. Mater. Sci. 4(2), 111–115. https://doi.org/10.1007/s11706-010-0024-1

[12] Ren, L., Lin, X., Tan, T., Yang, K. (2011). Effect of Surface Coating on Antibacterial Behavior of Magnesium Based Metals. Materials Letters, 65, 3509–3511. https://doi.org/10.1016/j.matlet.2011.07.109

[13] Cheng, A. Z. and Swaminathan, R., Layer By Layer (LbL) Self-Assembly Strategy

[14] And Its Applications, Nanotechnology Engineering, University of Waterloo, 1-5.

[15] Fekry, A. M., Tammam, R. H. (2012). Electrochemical Behavior of Magnesium Alloys as Biodegradable Materials in Phosphate Buffer Saline Solution. Int. J. Electrochem. Sci., 7, 12254-12261.

[16] Liuyun, J., Yubao, L. and Chengdong, X. (2009). A Novel Composite Membrane of Chitosan-Carboxymethyl Cellulose Polyelectrolyte Complex Membrane Filled with Nano-Hydroxyapatite I. Preparation and Properties. Journal of materials science. Materials in medicine, 20(8), 1645-1652. https://doi.org/10.1007/s10856-009-3720-6

[17] Gavoille, A. and Andremont, B. A. (1994). Measurement of Inhibition Zone Diameter in Disk Susceptibility Tests by Computerized Image Analysis. Computers in Biology and Medicine, 24(3), 179–188. https://doi.org/10.1016/0010-4825(94)90014-0

[18] Lalitha, M. K. (2003). Manual on Antimicrobial Susceptibility Testing. Indian Association of Medical Microbiologists, Report of an Intercountry Workshop India, 1-10.

[19] Jiang, L. (2011). Comparison of Disk Diffusion, Agar Dilution, and Broth Microdilution for Antimicrobials Susceptibility Testing of Five Chitosan. MS Thesis, Louisiana State University, Batonrougue, Louisiana.

[20] Wang, X., Du, Y., Fan, L., Liu, H. and Hu, Y. (2005). Chitosan- Metal Complexes as Antimicrobial Agent: Synthesis, Characterization and Structure-Activity Study. Polymer Bulletin, 55, 105–113. https://doi.org/10.1007/s00289-005-0414-1

[21] Kim, B. S., Park, S. W., Hammond, P. T. (2008). Hydrogen-Bonding Layer-by-Layer-Assembled Biodegradable Polymeric Micelles as Drug Delivery Vehicles from Surfaces. ACS Nano, 2(2), 386–392. https://doi.org/10.1021/nn700408z

[22] Noone, P. and Pattison, J. R. (1971). Therapeutic Implications of Interaction of Gentamicin and Penicillin. The Lancet, 298 (7724), 575–578. https://doi.org/10.1016/S0140-6736(71)80125-3

[23] Watanakunakorn, C. (1971). Penicillin Combined with Gentamicin or Streptomycin: Synergism against Enterococci. Oxford Journals Medicine, The Journal of Infectious Diseases, 124 (6), 6581-6586. https://doi.org/10.1093/infdis/124.6.581

[24] http://www.uphs.upenn.edu/bugdrug/antibiotic_manual/aminoglycosideresistance.htm, [cited March 20, 2017].

[25] Seraz, M.S. (2013) "Electrochemical Analysis of Antibacterial Polyelectrolyte Coated Mg Alloys for Cardiovascular Applications," M.S. Thesis, Wichita State University.

[26] Dunne, N., Buchanan, F., Hill. J., Newe, C., Tunney, M., Brady, A., Walker, G. (2008). *In vitro* Testing of Chitosan in Gentamicin-Loaded Bone Cement: No Antimicrobial Effect and Reduced Mechanical Performance. Acta Orthop, 79(6) 851-860. https://doi.org/10.1080/17453670810016957

[27] Spottel, S. and Darns, G. (1981). Pathogen Reduction in Closed Aquaculture Systems by UV Radiation: Fact or Artifact. Mar. Ecol. Prog. Ser., 6, 295-298. https://doi.org/10.3354/meps006295

[28] Maclean, M., MacGregor, S.J., Anderson, J.G. and Woolsey, G. (2009). Inactivation of Bacterial Pathogens following Exposure to Light from a 405-Nanometer Light-Emitting Diode Array. Appl Environ Microbiol, 75(7), 1932–1937. https://doi.org/10.1128/AEM.01892-08

[29] Seraz, S., Asmatulu, R., Chen, Z., Ceylan, M., Mahapatro, A., and Yang, S.Y. "Antibacterial Polyelectrolyte-Coated Mg Alloys for Biomedical Applications," SPIE Smart Structures/Non-destructive Evaluation Conference, San Diego, CA, March 9-13, 2014, 10 pages.

Received on 14-05-2017 Accepted on 19-05-2017 Published on 17-08-2017

DOI: https://doi.org/10.12974/2311-8741.2017.05.01.4

© 2017 Seraz *et al*.; Licensee Savvy Science Publisher.
This is an open access article licensed under the terms of the Creative Commons Attribution Non-Commercial License (http://creativecommons.org/licenses/by-nc/3.0/) which permits unrestricted, non-commercial use, distribution and reproduction in any medium, provided the work is properly cited.